Available online at www.sciencedirect.com
ScienceDirect
Procedia CIRP 66 (2017) 283 – 288
www.elsevier.com/locate/procedia

1st Cirp Conference on Composite Material Parts Manufacturing, cirp-ccmpm2017

# Lightweight design and manufacturing of composites for high-performance electric motors

Simon-Frederik Koch*, Manuel Peter, Jürgen Fleischer

*Karlsruhe Institute of Technology, wbk Institute of Production Science, Kaiserstraße 12, 76131 Karlsruhe, Germanny*

* Corresponding author. Tel.: +49-721-608-46019; fax: +49-721-608-45005. *E-mail address:* simon-frederik.koch@kit.edu

**Abstract**

The global demand for carbon saving and green mobility is changing propulsion systems from combustion engines to electric motors. Today, battery capacities are still low and the range of automotive vehicles needs to be improved. In this context, high-performance electric motors of high energy efficiency as well as low weight are gaining in importance.
In the present paper, two approaches for reducing weight of electric motor rotors are presented. First, a lightweight approach comprising a hybrid shaft made of carbon reinforced plastic and stainless steel are outlined. It is manufactured by a novel process chain, where dry filament winding is combined with centrifugal casting. The steel inlays are joined in-mold during centrifugal casting. The second approach demonstrates the replacement of electric sheets by soft magnetic compounds (SMC, iron filled polyamide compound). These SMC parts are produced in an innovative two-component injection molding process. The paper concludes with a concept for the assembly of the hybrid shaft with the SMC parts and the mechanical testing of the assembled lightweight rotor.


Peer-review under responsibility of the scientific committee of the 1st Cirp Conference on Composite Materials Parts Manufacturing

*Keywords:* electric motor; shaft; carbon; reinforced plastic; centrifugal casting; rotational molding;

## 1. Introduction

Electric motors are constantly being improved due to progressing automation of production systems and the transition from combustion engines to electric drives. Manufacturers and suppliers of electric automotive drive technology must be capable of developing, designing and economically producing required key components, such as the electric drive engine, in an efficient way that is also flexible in its application in series production. Essential adjustable factors constitute in reducing power dissipation and thus increasing efficiency of the electric drive.

The integration of lightweight technology based on fiber reinforced plastics, such as for example carbon fiber reinforced plastics (CFRP), offers the highest potential for reducing the weight of electric drive trains while at the same time improving the electrical and mechanical properties of the drive systems. For electric traction drives, as they are installed in cars, robots or portals, for example, the objective also constitutes in reducing the rotor's mass inertia in addition to general weight reduction. This aims at achieving higher accelerations which positively affects the dynamics or productivity. It is due to high power density and precise controllability that permanent magnet synchronous motors (PMSM) are particularly suited for being used as traction drives in electric vehicles [1, p 579], [2]. This article thus presents two novel approaches for weight reduction in rotors of PMSM.

## 2. State of the art

### *2.1. Design of permanent magnet rotors*

Rotors of PMSM always comprise at least the components: rotor shaft, magnet carrier, permanent magnet (PM) and


Peer-review under responsibility of the scientific committee of the 1st Cirp Conference on Composite Materials Parts Manufacturing
doi:10.1016/j.procir.2017.03.274

magnet fixation (Fig. 1) [3]. Additional components might be required for fixing the magnet carrier or balancing the rotor such as for example balancing plates or clamping elements.

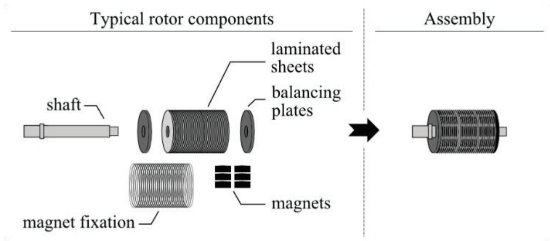


Fig. 1. Components of a permanent magnet rotor.

When dealing with a PMSM with 75 kW continuous power and a rotor weight of 8.7 kg, the magnet carrier accounts for 61 % of the total weight, the rotor shaft for 30 %, the permanent magnets for 16 % and other components for 2 % [4]. The heavy weight of the components results mainly from the materials used.

The magnet carrier is assembled with electric sheets of a high magnetic permeability $\mu_r$ and a density of approx. 7600 kg/m³ [5]. It is by a separation process that the electric sheets are cut, then stacked on top of one another until they have reached the desired length and subsequently joined together. The electric sheet consists of soft magnetic material with electrically insulating coating. The insulating layer is important for reducing the eddy current losses. Due to the coating, a small gap between the sheets arises which is not filled with magnetic conductive material. If the sheet surface of the cross section is put into relation to the total surface of the cross section, the lamination factor can be calculated, usually, it amounts to 0.97 to 0.98 [6]. The density of the sheet package is thus only slightly smaller than the one of a massive steel component.

The rotor shaft for internal rotors is manufactured by machining from solid metal and in some instances by internal high-pressure forming [3], [7]. In both cases, the used material is steel (density of approx. 7850 kg/m³). Repercussions of the rotor shaft on dynamics are minor because of the low radial expansion of the rotor shaft. For this reason, hollow shafts are not installed in numerous applications.

### *2.2. Conventional production of permanent magnet rotors*

For the purpose of assembling the rotor, the magnets are mounted onto the magnet carrier made of electric sheet which in turn is connected to the shaft [8]. When it comes to mounting the magnets, a distinction is made between surface mounted and buried magnets. Surface mounted magnets are either joined in radial direction or inserted in axial direction into form-fit pockets [9]. Due to their design, buried magnets are always inserted in axial direction into the magnet carrier. Typically, the fixation of the magnets is performed by adhesive bonds [10]. Other types of fixation constitute in caulking or clamping [11]. Depending on the operating conditions, an outer bandage is used as additional fixation for surface mounted magnets. Typical bandages are yarn bandages made of carbon fiber reinforced plastics or thin, cylindrical sleeves made of stainless steel [11]. The magnet carrier and the balancing plates are connected in a force-locking or form-fitting manner to the rotor shaft. Common processes constitute in shrinking the shaft or pressing a knurled shaft [11].

### *2.3. Soft magnetic composites*

Soft magnetic composites (SMC) have been developed for guiding the magnetic flux at the cost of smallest eddy current losses. They consist of ferrous particles (particle size approx. 100 µm) with a high magnetic remanence $\mu_r$. The particles in the SMC material can be electrically conductive to each other (first generation material) or they can be electrically insulated (second generation material) [12]. Since the particles are insulated from one another, there are hardly any eddy current losses in the material. Consequently, SMCs are outstandingly suitable for applications in quickly switching coils, sensors and in particular electric drives [13].

The processing of the material has so far been limited to processes of pressing, powder metallurgy and metal injection molding [14]. A binder that needs to be removed in a sinter process is used for the execution of these procedures [15].

### *2.4. Carbon fiber reinforced plastic shafts*

Carbon fiber reinforced plastics (CFRP) demonstrate excellent specific rigidity and strength properties. They are thus suitable for manufacturing hollow CFRP shafts. The hollow construction allows for excellent material utilization since it is characterized by a high geometrical moment of inertia and low weight.

Today, CFRP shafts are mainly manufactured by wet winding. In this process, dry yarn is pulled through a resin bath and wound onto a rotating mandrel. The winding patterns can flexibly be adapted to the arising loads. The component is cured in an oven. Afterwards, the CFRP shaft must be removed from the mandrel [16]. During wet winding, the wet rovings that are wound onto one another must feature uniform frictional and adhesive properties. The steady pace can only be achieved with slow-reacting resin hardening systems. The results are long cycle times and a reduction of productivity of the process [17].

Subsequently, the CFRP shaft is connected to the metal elements. The metal introduces the load into tribological highly-stressed areas as they occur in bearings or gear wheels. The CFRP area transfers the loads over long distances and essentially reduces the weight (compared to a steel shaft).

Suitable joining technologies constitute in subsequent adhesion [18], interface fit assembly [19], screw or bold connections [20] and polygonal couplings [21, 22].

## 3. Approach: Composites in lightweight rotors

This article examines two new technologies where a magnet carrier of SMC material is shoved onto a hybrid shaft of CFRP and steel. Both technologies pursue the objective of reducing weight and facilitating flexible and scalable manufacturing.

The basic design of a rotor with both technologies is depicted in Fig. 2 and is explained in the following.

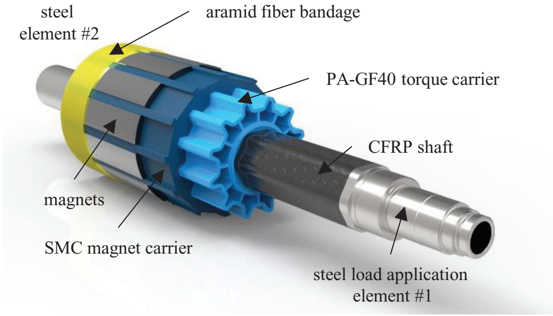


Fig. 2. Concept of a lightweight PM rotor made of composites

The hybrid rotor is fitted with steel elements on both ends to support the ball bearings and a shaft encoder and to serve as a connection for a coupling or a gear box. As a result, conventional assembly processes, as they are used for pure metal shafts, may be applied and defective or worn components can easily be replaced.

A polygonal coupling with rounded edges positively connects the CFRP shaft to both steel elements. The CFRP shaft covers the entire length of the electro-magnetic active part of the rotor (240 mm). The same polygonal contour is adopted by the carrier which in turn also leads to a positive torque transmission.

Multiple carriers are equipped with 12 magnets per carrier, shoved onto the shaft and axially fastened with a shaft nut (not illustrated). Lastly, a bandage of aramid fibers which absorb the magnets' centrifugal forces during operation is wound around the component.

In the following sections, the hybrid CFRP steel shaft (Sec. 4) and the magnetic carrier (Sec. 5) are described in more detail.

## 4. Results: Hybrid CFRP metal rotor shaft

### *4.1. Design and Dimensioning*

Finite element simulations were carried out for dimensioning the CFRP steel shaft. The steel inserts have been modeled with a linear elastic material model and the CFRP laminate with the help of the classic laminate theory and an orthotropic material law. A balanced angle-ply laminate with $\pm 45°$ was used for transferring the torsion moments. With a laminate thickness of 3 mm, this structure, however, expands elastically in the overlapping area. This reduces the load-bearing capacity. It is a behavior that can be minimized by introducing circumferential windings with around 90° fiber orientation [23]. In this work, they were specified at 2 mm.

The polygon shape is interesting for the form-locking load transfer between steel insert and CFRP. A parameter study was carried out to analyze the influence of the number of edges on the tensions in the connection and in the laminate. During this, an epicycloidal polygon shape was chosen [24] and the nominal radius of the profile was linked to the eccentricity in order to obtain convex shapes at all times. This approach guarantees the demoldability of the CFRP shaft. Such profile shapes can be described as follows:

$$\binom{x}{y} = \begin{pmatrix} r_a \left[1 - \frac{1}{(n+1)^2+1}\right] cos\, \alpha + \frac{r_a}{(n+1)^2+1} cos(n+1)\, \alpha \\ r_a \left[1 - \frac{1}{(n+1)^2+1}\right] sin\, \alpha + \frac{r_a}{(n+1)^2+1} sin(n+1)\, \alpha \end{pmatrix} \quad (1)$$

The polygon shape with its coordinate x,y are represented by the number of edges $n$ and the pitch circle radius $r_a$. The variable $\alpha$ is the local angle coordinate.

The ideal number of edges was determined by simulating the CFRP failure modes with Hashin's criterion [25] and by analyzing the contact shear stress between CFRP shaft and steel insert. This way, laminate stress and adhesive properties of the co-cured bonding are modelled. Fig 3. shows the results of the parameter study from three edges up to ten. Higher edge numbers are not suitable as the resulting connection is converging to a cylindrical shape. The contact shear stress peak at 8 edges can be explained by the locally higher edge radius.

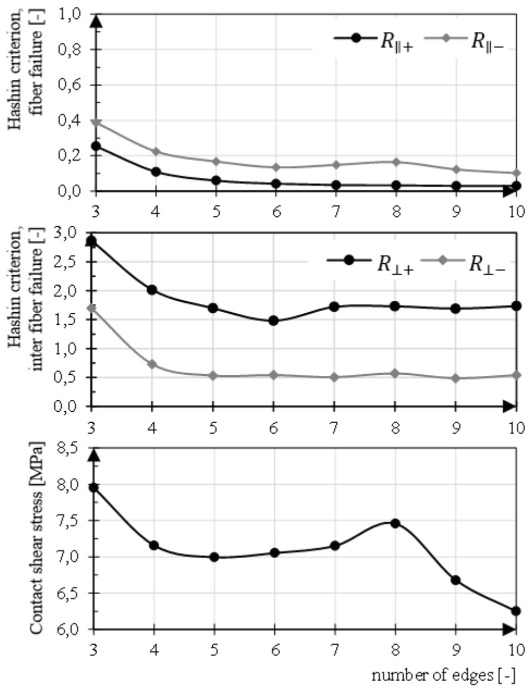


Fig. 3. Influence of number of edges on laminate failure & adhesive shear stress

According to Fig 3 the four hashin failure criteria (fiber tension, fiber compression, matrix tension, matrix compression) and the shear stress have lowest values for five or six edges. For an easy demoldability an even number of edges is favorable. Consequently, six edges were chosen in further investigations.

The load-bearing capacity of this hybrid shaft concept was proved by mechanical torque tests. All shafts transmitted up to 400 Nm torque, which ensures a factor of safety of 1.5.

### *4.2. Dry filament winding and centrifugal casting*

A new multistage process chain was developed for producing the rotor shaft. This process chain consists of a dry winding process to manufacture a dry fiber preform which is impregnated by centrifugation. Both processes can be performed automatically on a turning center.

Fig. 4 shows the sequence for producing the preform in a dry winding process.

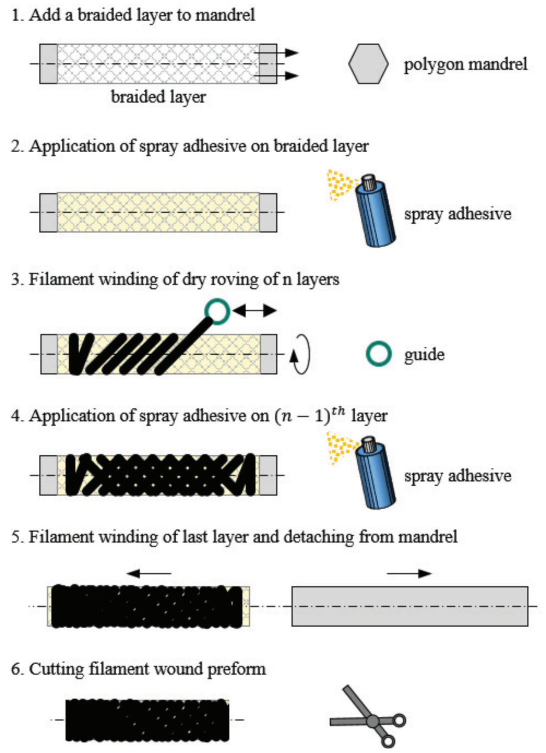


Fig. 4. Process chain for manufacturing of CFRP metal hybrid rotor shafts by dry filament winding and centrifugal casting

In order to manufacture a polygon-shaped CFRP shaft, the preform must be wound with a pattern that is close to the final contour and appropriate to the load. For the winding process, a polygon-shaped mandrel coated with teflon (PTFE) is required. The teflon reduces the friction between fiber preform and mandrel and, it allows for the low-force and non-destructive removal of the preform from the mandrel.

The first step (Fig. 4, 1) involves the application of a thin glass-fiber (GF) braided sleeve onto the mandrel. The GF sleeve has two functions: It supports the non-destructive removal of the finished preform from the mandrel (5) and protects the metal adjacent to the CFRP from corrosion.

In order to sufficiently connect the GF sleeve with the wound layers, the sleeve is lightly moistened with spray adhesive prior to the winding process (2/4). Subsequently, the winding process starts (3) and the spraying of adhesive after each layer may continue. This enhances the stability and stiffness of the manufactured preforms which is of advantage for the subsequent trimming. Applying too much spray adhesive in turn reduces the permeability of the fiber structure when impregnated during the centrifugal casting [26]. Flow barriers causing dry spots in the laminate could be the result.

Own works have shown that, for the combined process chain of dry wound preforms and their impregnation by centrifugal casting, it is sufficient to spray only the first braided layer (2) and the penultimate wound layer with adhesive. The preform can be cut to length under these circumstances with only a few fiber disorientations at the edges (6) and, moreover, has a sufficient inherent rigidity for further processing. The trimmed preform is subsequently impregnated by centrifugal casting. During this procedure, also the load-bearing metallic elements shall be intrinsically [27] joined with one another (see Fig. 5).

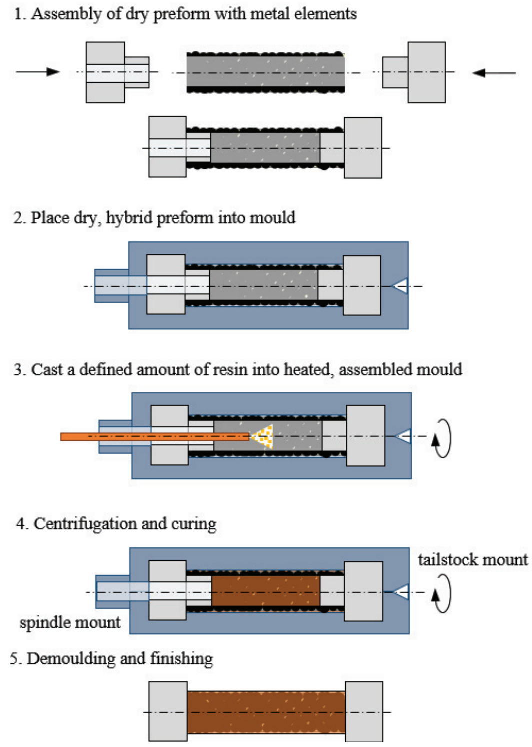


Fig. 5. Process chain of centrifugal casting and intrinsic joining for CFRP-metal rotor shafts

After trimming the preform, the metallic load-bearing elements are pushed into the preform (Fig. 5, 1) and the evolving hybrid dry preform is put into the tool for centrifugal casting (2). To ensure fast hardening, the mold should be preheated (3).

As soon as the mold reaches the desired temperature, the centrifugation can be started. For this purpose, the mold is fixed into a centrifugation device (e.g. lathe, turning center). Now, the mold can be set into rotation and the liquid tempered mixture of resin and hardener poured via a lance (3) into the mold.

It should be noted that only a defined amount of resin $m_m$ is poured into the mold during the centrifugal process [SFK6].

$$m_m = \rho_m V_m = \rho_m(1-\varphi_f)V \qquad (2)$$

The amount of resin depends on the density of the matrix $\rho_m$ and the matrix volume $V_m$, that in turn can be replaced by the fiber volume content $\varphi_f$ and the total volume $V$ of the CFRP shaft. Higher amounts of resin might generate a circular resin-rich layer inside. Low amounts might cause incomplete impregnation and dry spots in the laminate.

Moreover, sufficiently high centrifugal forces are required for the rotation so that the resin fully applies to the inside of the preform and impregnates it during the process. Therefore, a minimum rotational speed is necessary to compensate the weight force action. In order to reach high laminate qualities and fiber volume contents, however, it is rotated at a much higher speed [28]. The rotation is continued until the matrix is fully impregnated and the resin is cured (4). Finally, the hybrid shaft can be removed from the mold and, if necessary, can be reworked (5).

By pushing the metal elements into the fiber preform the impregnation of the fiber structure is combined with an in-mold assembly of the metal. The resulting connection has form-fitting parts due to the polygon, substance-to-substance bonded parts because of the co-cured bonding of the matrix and force locked parts due to the curing and therefor inherent tension that can all contribute to the load transfer.

The short paths of flow and impregnation allow for using highly reactive resin systems. These systems provide fast curing and therefore short cycle times under 20 minutes. With a three-shift operation and 250 workdays per year, 18,000 shafts can be produced. Compared to a conventional solid steel shaft this technology is offering about 50% mass reduction.

## 5. Results: Magnet carrier made of soft magnetic compound

The developed magnet carrier meets the required functional separation of the torque transmission and the magnetically active part by using a new innovative structure. The linking with the turning moment is realized by a glass fiber reinforced plastic material. The flow of the magnet field is conducted by a material made of SMC (Fig. 6, a).

The length of the magnet carrier and of the permanent magnets was chosen in a way that the magnet carrier presents the same length as the magnet. For the design of a complete rotor, multiple magnet carriers loaded with magnets are pushed axially onto the rotor shaft. For a safe torque transmission and an easy assembly, a form-fitting connection between magnet carrier and rotor shaft was selected.

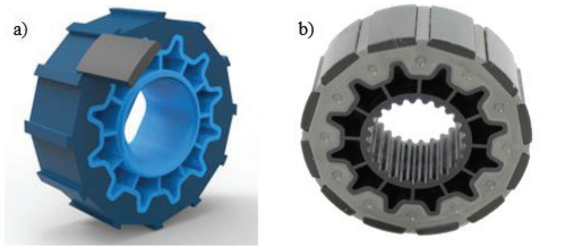

Fig. 6. a) Visualization of the magnet carrier consisting of two injection molded components: SMC (dark blue) and PA (light blue), b) Depiction of a single rotor disc with mounted magnets but without fiber bandage.

A Fe-Ni material with high magnetic permeability $\mu_r$ was chosen as SMC material which was then compounded in a polyamide (PA) plastic with a filling degree of approximate 57 %. Due to the PA matrix, the soft magnetic particles were provided with enough stability for later operation. The particle size of the soft magnetic material was chosen to be smaller than 100 µm to achieve a uniform distribution within the matrix. FEM simulations and form fill simulations ensured the product characteristics as well as the producibility. The weight of the magnet carrier merely amounts to 398 g.

The technology needed for production is a conventional injection molding machine with a specific injection mold. The process itself is very suitable for mass production. In contrast to the conventional MIM process, no binder material needs to be removed. Thus, the time and complexity of the process as well as the cost is reduced. After the process of injection molding, the components can be used immediately. The cycle time for manufacturing a disc is 170 s. The annual output (see assumptions in Sec. 4) calculates to 127,000 magnet carriers. The cycle time can be reduced even more by using a tool/mold with two, four or more cavities.

An examination of the material in a scanning electron microscope (SEM) reveals a homogenous particle distribution inside the matrix and good insulation of the particles against each other (Fig. 7).

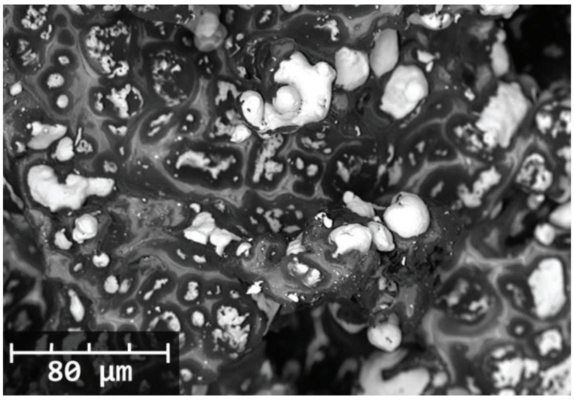


Fig. 7. SEM photo of injection molded SMC material. Light areas: Iron particles. Dark areas: PA plastic material.

A positive locking clearance fit (dovetail) for mounting the magnets is located in the outer part of the magnet carrier. The fit merely serves as an assembly aid. For reaching the required operational stability, the magnets are adhesively bonded onto it and secured by a fiber bandage (Fig. 6, b).

## 6. Summary & Conclusion

Considering the mass distribution on component level of a traction drive reveals two components with the highest mass in the rotor: the metal rotor shaft (approx. 30 % of total rotor weight) and the laminated magnet carrier (approx. 61 % of total rotor weight). Improving weight and inertia of these parts leads to benefits in overall motor mass and dynamic, as demanded by many automobile manufactures. Replacements with reduced mass, inertia and improved electro-magnetic properties are investigated for both components. The development of a prototype manufacturing process ensures the industrial producibility.

The replacement for the rotor shaft is a hybrid carbon fiber reinforced plastic shaft. The required production processes are investigated in this paper. The combined dry filament winding process for preforming and the impregnation by a rotational molding process is capable of producing 18,000 parts per year.

The replacement for the magnet carrier is an injection molded SMC part with a functional separation of the torque transmission and the magnetically active part. A standard injection molding machine with two injection units and a special mold are sufficient. This simple setup already allows the production of 127,000 magnet carriers per year.

## Acknowledgements

We wish to extend out special gratitude to the Federal Ministry of Economic Affairs and Energy (BMWi) for its support of the project "ProLemo – Produktionstechnologien für effiziente Leichtbaumotoren für Elektrofahrzeuge".

## References

[1] Emadi, A. (2005): Handbook of automotive power electronics and motor drives. Boca Raton: Taylor & Francis, (Electrical and Computer Engineering 125)

[2] Benjamin, F.; Klötzke, M.; Kreyenberg, D. (2015): Begleitforschung zu Technologien, Perspektiven und Ökobilanzen der Elektromobilität: STROMbegleitung. Abschlussbericht.

[3] Kampker, A.; Burggraf, P.; Nee, C. (2012): Costs, quality and scalability: Impact on the value chain of electric engine production. In: 2nd International Electric Drives Production Conference (EDPC), p. 1–6

[4] Peter, M.; Fleischer, J.; Blanc, F. S. L.; Jastrzembski, J. P. (2013): New conceptual lightweight design approaches for integrated manufacturing processes: Influence of alternative materials on the process chain of electric motor manufacturing. In: Electric Drives Production Conference (EDPC), 3rd International, p. 1–6

[5] Cogent Power, Material Data Sheet, 04.01.2017, http://cogent-power.com/cms-data/downloads/Cogent%20NO%20brochure%202016.pdf

[6] Kulkarni, S. V.; Khaparde, S. A. (2013): Transformer engineering : Design, technology, and diagnostics. 2nd ed. Boca Raton, FL : CRC Press, Taylor & Francis Group

[7] Yuan, S. J.; Liu, G. (2014): Tube Hydroforming (Internal High-Pressure Forming). In: Comprehensive Materials Processing : Elsevier, p. 55–80

[8] Franke, J.; Tremel, J.; Kühl, A. (2011): Innovative developments for automated magnet handling and bonding of rare earth magnets. In: Assembly and Manufacturing (ISAM), 2011 IEEE International Symposium on, p. 1–5

[9] Wang, J.; Yuan, X.; Atallah, K. (2013): Design Optimization of a Surface-Mounted Permanent-Magnet Motor With Concentrated Windings for Electric Vehicle Applications. In: IEEE Transactions on Vehicular Technology 62, Nr. 3, p. 1053–1064

[10] Gieras, J. F.(2011): Permanent Magnet Motor Technology: Design and Applications, Third Edition : CRC Press, Electrical and computer engineering

[11] Mahr, A.; Meyer, A.; Hofmann, B.; Masuch, M.; Franke, J. (2015): Innovative developments for automated assembly and fixation of integrated permanent magnets in rotors of synchronous machines. In: Electric Drives Production Conference (EDPC), 5th International, p. 1–6

[12] Bas, J.A.; Calero, J.A.; Dougan, M.J. (2003): Sintered soft magnetic materials. Properties and applications. In: Journal of Magnetism and Magnetic Materials 254-255, p. 391–398

[13] Hultman, L. O.; Jack, A. G. (2003): Soft magnetic composites-materials and applications. In: International Electric Machines & Drives Conference, p. 516–522

[14] Heaney, Donald F. (2012): Handbook of metal injection molding. Cambridge, UK, Philadelphia, PA : Woodhead Publishing

[15] Miura, H. (2012): Metal injection molding (MIM) of soft magnetic materials. In: Handbook of Metal Injection Molding : Elsevier, S. 487–515

[16] Henning, F.; Moeller, E. (Hrsg.) (2011), Handbuch Leichtbau. Methoden, Werkstoffe, Fertigung, Hanser, München. http://www.hanser-elibrary.com/isbn/9783446422674. ISBN: 978-3-446-42891-1

[17] Wang, R.; Jiao, W.; Liu, W.; Yang, F.; He, X. (2011), „Slippage coefficient measurement for non-geodesic filament-winding process", Composites Part A: Applied Science and Manufacturing, Bd. 42, Nr. 3, S. 303–309.

[18] Kim, K.S.; Kim, W.T.; Lee, D.G. (1992): Optimal tubular adhesive-bonded lap joint of the carbon fiber epoxy composite shaft, Volume 21, Issue 3, pp. 163-176, doi:10.1016/0263-8223(92)90016-6

[19] Kim, S. S.; Lee, D. G. (2006), „Design of the hybrid composite journal bearing assembled by interference fit", Composite Structures, Bd. 75, 1-4, pp. 222–230.

[20] Cho, H.D.; Lee, D.G.; Choi, J.H. (1997): Manufacture of one-piece automotive drive shafts with aluminum and composite materials, Composite Structures, Volume 38, Issue 1-4, pp. 309-319, http://dx.doi.org/10.1016/S0263-8223(97)00065-2

[21] Fleischer, J.; Koch, S.F.; Coutandin, S.: Manufacturing of polygon fiber reinforced plastic profiles by rotational molding and intrinsic hybridization, S. Prod. Eng. Res. Devel. (2015) 9: 317. doi:10.1007/s11740-015-0620-0

[22] Hufenbach, W.A.; Helms, O.; Werner J. (2007) Shaft to collar connections for high loaded composite lightweight gear components. Welle-Nabe-Verbindungen: Berechnung, Gestaltung, Anwendung, VDI-Berichte Nr. 2004

[23] Hufenbach, W.A. et al (2005): Integrated pipe thread for the introduction of high loads into filament wound lightweight structures. In: VDI-Berichte (1903): Berechnung, Gestaltung, Anwendung, Schraubenverbindungen, pp. 301–316

[24] Ziaei, M. (2007): Flexible Continuous Interior and Outer Contours for Form- and Force- Closured Connections on the Basis of Complex Cycloids, VDI-Berichte Nr. 2004, pp. 277-294

[25] Hashin, Z. (1980): Failure Criteria for Unidirectional Fiber Composites, J. Appl. Mech 47(2), pp. 329-334, doi:10.1115/1.3153664

[26] Endruweit, A.; Long, A.C. (2010): Analysis of Compressibility and Permeability of Selected 3D Woven Reinforcements, Journal of Composite Materials, Vol 44, Issue 24, pp. 2833-2862, DOI: 10.1177/0021998310369586

[27] Fleischer, J.; Ochs, A.; Dosch, S. (2012): The future of lightweight manufacturing - production-related challenges when hybridizing metals and continuous fiber-reinforced plastics, Proceedings of International Conference on New Developments in Sheet Metal Forming, May 22nd - 23rd 2012, Stuttgart, pp. 51–70.

[28] Neitzel, M.; Mitschang, P. (2004): Handbuch Verbundwerkstoffe - Werkstoffe, Verarbeitung, Anwendung; Carl Hanser Verlag; Kaiserslautern; pp. 329-333